Embedded Current-Fed Switched-Z-Source Inverters

Mohsen Hasan Babayi Nozadian, *Student Member, IEEE*, Ebrahim Babaei, *Senior Member, IEEE*, Seyed Hossein Hosseini, *Member, IEEE,* Vida Ranjbarizad

Faculty of Electrical and Computer Engineering, University of Tabriz, Tabriz, Iran
m.hasanbabayi@tabrizu.ac.ir, e-babaei@tabrizu.ac.ir, hosseini@tabrizu.ac.ir, vidaranjbarizad@yahoo.com

Abstract

In this paper, two new structures for embedded current-fed switched-Z-source inverters (ECSZSIs) are proposed. The proposed inverters can generate high output current from low input current and they have a good immunity against the open circuit of the legs and electromagnetic interference (EMI). The proposed structures have the less number of passive elements in comparison with the conventional current-fed Z-source inverter (CZSI) to generate the same current boost factor. In addition, the proposed structures have the continuous input voltage. Complete analyses of the performance of the proposed structures in different operating modes are presented and the voltages and currents equations of all elements are calculated. Moreover, the switching pattern based on pulse width modulation (PWM) is proposed. The comparison between the proposed inverters and conventional CZSI is presented, too. Finally, the simulation results using PSCAD/EMTDC software are presented to reconfirm the accuracy of theoretical analyses and obtained equations.

Keywords—Switched-Z-source inverter, Current-Fed Z-source inverter, Current source inverter, Voltage source inverter.

1. Introduction

Similar to conventional voltage source inverter (VSI) and current source inverter (CSI), Z-source inverters (ZSIs) are based on voltage source and current source, too. VSI cannot increase the level of input voltage and also CSI cannot increase the input current level at output. In addition, VSI has a problem when short-circuit occurs in its legs and CSI has a problem when open-circuit occurs in its legs. In order to resolve these problems, the Z-source inverters based on voltage and current sources have been presented in literatures that are good alternative for VSI and CSI, respectively.

In [1], the conventional ZSI with voltage source and current source has been presented that it uses from an X-shape Z-source network. The Z-source inverter with voltage source is immune to shoot-through and the Z-source inverter with current source (CZSI) does not have problem when the legs of inverter are open-circuit. According to the unique features of the Z-source inverters, numerous papers have been published related to these converters. In some of these papers, new structures have been presented [2-4]. On the other hand, the control methods of Z-source inverters have been introduced in [5,6]. The Z-source inverters have many applications in renewable energy systems [7,8], micro-grids [9], and electrochemical applications [10]. In some of papers, the operation of CZSI has been presented. In [11], the different PWM control methods for CZSI have been presented. In [12], the careful integration of three-step compensators before the pulse width modulator of inverter has been presented for damping triggered resonant oscillations.

In this paper, two new structures are proposed for switched-Z-source inverters with current-fed. The proposed structures have less passive elements in comparison with CZSI. The current boost factor of ECSZSIs is equal to current boost factor of CSZSI and voltage across input source in the proposed structures is continuous. The performances of proposed structures are presented in different operating modes and the voltage and current equations of proposed inverters are calculated, too. The comprehensive comparison between proposed inverters and conventional structures is provided.

2. Proposed structures

The power circuits of the proposed structures are shown in Fig. 1. Figs. 1(a) and 1(b) show the type I and type II of the proposed structures, respectively. According to Fig. 1, the proposed topologies have two passive elements and three semiconductors switches. The type I and type II have some differences. In type I, the inductor L has common node with the emitter of switch S. In type II, the inductor L has common node with collector of switch S. In addition, the current source in type I has common ground with inverter stage while in type II, there is no common ground between current source and inverter stage. In the proposed structures, unidirectional-current bidirectional-voltage switches are used that one kind of these switches is shown in Fig. 1. Each switch consists of series connection of one diode and one insulated gate bipolar transistor (IGBT). The Z-source inverters based on current source have open-circuit duty cycle (D_{OC}). This duty cycle is calculated from ratio of open-circuit time interval to the time interval of a switching period. According to the value of D_{OC}, it is possible to increase or decrease the output current of converter. The proposed inverters have two operating modes named open-circuit (OC) mode and none open-circuit (nOC) mode, respectively. In the following, the performances of ECSZSIs in two operating modes are presented.

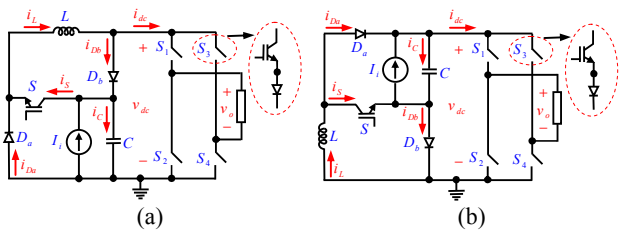

Fig. 1. Power circuits of the proposed topologies; (a) type I; (b) type II

2.1. Analyses the Proposed Structures in OC and nOC Modes

In OC mode, the switch S and the switches of inverter stage ($S_{i=1to4}$) are turned off and the diodes D_a and D_b are turned on. The equivalent circuits of this operating mode for the type I and type II are shown in Fig. 2. According to Fig. 2, the legs of the inverter are open-circuit, so, power does not transfer to load. In addition, the input voltage is equal to the voltage across of capacitors and the value of input voltage is not zero.

In this operating mode, the switches S and S_i are turned on and the diodes D_a and D_b are turned off. In nOC mode, the current source with inductor feeds the load. The equivalent circuits of type I and type II of ECSZSI in nOC mode are shown in Figs. 3(a) and 3(b), respectively.

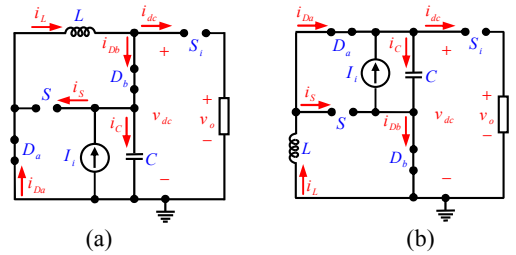

Fig. 2. Equivalent circuits of the proposed structures in OC mode; (a) type I; (b) type II

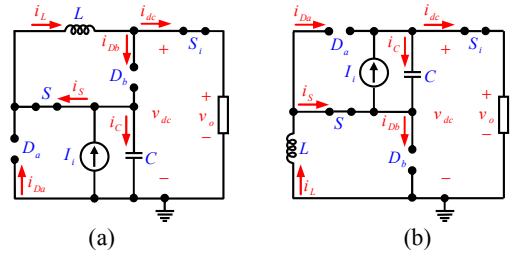

Fig. 3. Equivalent circuits of the proposed structures in nOC mode; (a) type I; (b) type II

If the values of inductors and capacitors are assumed large, so, the current ripple of inductor and voltage ripple of the capacitor can be ignored in comparison with their average values. By applying KVL and KCL in equivalent circuits, the voltage and current equations of all elements in OC and nOC modes are calculated as follows:

$$i_C = \begin{cases} I_i + I_L & OC \\ I_i - I_L & nOC \end{cases} \quad (1)$$

$$v_L = \begin{cases} -V_C & OC \\ V_C - v_{dc} & nOC \end{cases} \quad (2)$$

$$i_S = \begin{cases} 0 & OC \\ I_L & nOC \end{cases} \quad \& \quad v_S = \begin{cases} V_C & OC \\ 0 & nOC \end{cases} \quad (3)$$

$$i_{Da} = \begin{cases} I_L & OC \\ 0 & nOC \end{cases} \quad \& \quad v_{Da} = \begin{cases} 0 & OC \\ -V_C & nOC \end{cases} \quad (4)$$

$$i_{Db} = \begin{cases} I_L & OC \\ 0 & nOC \end{cases} \quad \& \quad v_{Db} = \begin{cases} 0 & OC \\ v_{dc} - V_C & nOC \end{cases} \quad (5)$$

where I_L indicates the average current of inductor and V_C shows the average voltage across capacitor.

According to equations (1) to (5) and in OC mode, the current of capacitor is equal to sum of input current and current through of inductor, so, in this operating mode the inductor charges the capacitor. In addition, in this operating mode, the voltage across inductor is negative and is equal to capacitor voltage. The current through the switch S is equal to zero and its voltage is equal to the voltage across capacitor. Furthermore, the voltages across diodes are equal to zero because they are turned on.

In nOC mode, the value of I_L is always greater than I_i; therefore, the value of i_C is negative and the capacitor is discharged. In addition, the switch S is turned on, so, its voltage is equal to zero. The currents through of diodes are equal to zero because they are off.

According to the above equations and the equivalent circuits, the voltage and current of dc-link are calculated as follows:

$$i_{dc} = \begin{cases} 0 & OC \\ I_L & nOC \end{cases} \quad \& \quad v_{dc} = \begin{cases} V_C & OC \\ Ri_{dc} & nOC \end{cases} \quad (6)$$

Considering the equivalent circuits and the obtained equations, it is clear that in this operating mode the voltage and current equations of all elements are same for both types. Voltage and current waveforms of the proposed inverters in steady state are shown in Fig. 4. It should be noted that the gates signals in Fig. 4 have been obtained by the proposed switching pattern that it is introduced in next section.

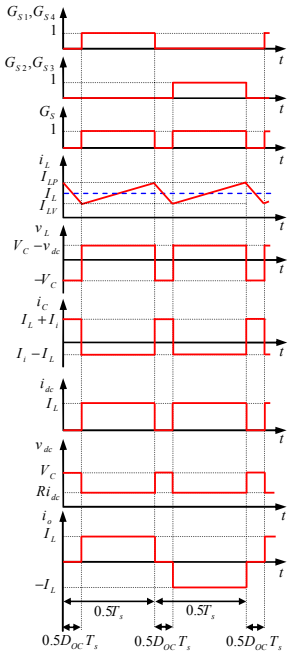

Fig. 4. Key waveforms of the proposed inverters

2.2. Calculation of Current Boost Factor

In the steady state, the average current of capacitor is equal to zero. Therefore, according to the values of i_C from (1), the average value of inductor current is calculated as follows:

$$I_L = \frac{1}{1-2D_{OC}} I_i \tag{7}$$

The value of current boost factor (B_I) is achieved from the ratio of the maximum value of dc-link current ($i_{dc,\max}$) to the value of the input current, so we can write:

$$B_I = \frac{i_{dc,\max}}{I_i} = \frac{I_L}{I_i} = \frac{1}{1-2D_{OC}} \tag{8}$$

According to the value of i_{dc} from (6) and the value of I_L from (7), the average value of dc-link current is calculated as follows:

$$I_{dc} = \frac{1-D_{OC}}{1-2D_{OC}} I_i \tag{9}$$

The maximum value of the output voltage for resistive load is obtained as follows:

$$v_{o,\max} = Ri_{o,\max} = RI_L \tag{10}$$

Furthermore, by considering the voltage balance law in inductors and according to the value of v_L from (2), the average voltage of capacitor is calculated as follows:

$$V_C = \frac{1-D_{OC}}{(1-2D_{OC})^2} RI_i \tag{11}$$

3. Proposed switching pattern

In this section, a suitable PWM technique for ECSZSIs and the generation of gates signals is proposed.

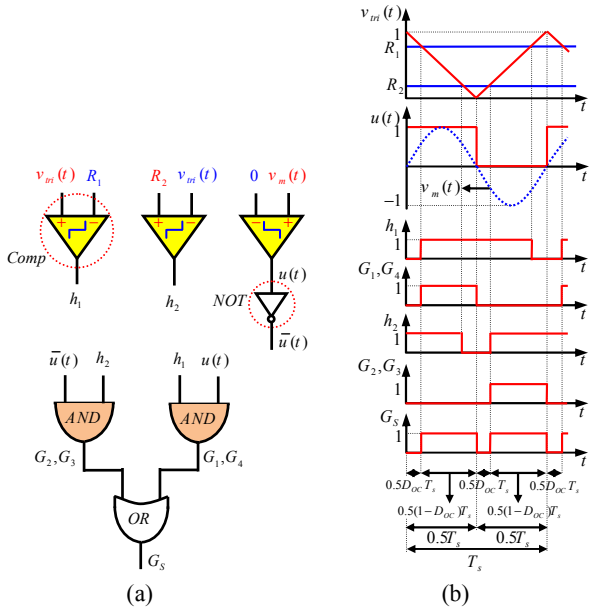

(a) (b)

Fig.5. (a) Logical diagram of proposed PWM control method; (b) Control signals in OC and nOC modes

Fig. 5(a) shows the logical diagram of the proposed PWM method. According to Fig. 5(a), the OC state is created by using two reference signals (R_1, R_2), one triangle signal ($v_{tri}(t)$), and one sinusoidal signal ($v_m(t)$). In addition, the waveforms of control signals in OC and nOC modes are shown in Fig. 5(b). Generation of gates signals and equations between the references signals and the duty cycle are shown in Table 1. In Table 1, "$\wedge$" and "$\vee$" denote logical "AND" and "OR", respectively.

Table 1. Equation of signals' gates

$R_1 = 1 - D_{OC}$	$R_2 = D_{OC}$
$G_1 = G_4 = h_1 \wedge u(t)$	$G_2 = G_3 = h_2 \wedge \bar{u}(t)$
$G_S = G_1 \vee G_2$	

4. Current ripple of inductor and voltage ripple of capacitor

Despite of this point that the voltage of capacitor and the current of inductor have been considered constant; however, in real system they have ripple. The current ripple of inductor and voltage ripple of capacitor are important in design of the values of inductor and capacitor. In addition, by increasing the ripples of current and voltage, the current and voltage stresses on elements are increased. The following equation is always true between the voltage and current of an inductor:

$$v_L = L\frac{di_L}{dt} = L\frac{|I_{LPP}|}{\Delta t} \tag{12}$$

where $I_{L,PP}$ indicates the current ripple of inductor.

Considering the values of v_L from (2) and V_C from (11), the current ripple of inductor is calculated as follows:

$$|I_{L,PP}| = \frac{D_{OC}(1-D_{OC})RI_i}{2Lf_s(1-2D_{OC})^2} \tag{13}$$

According to above equation, it is clear that the current ripple of inductor is directly proportional to I_i and R. Also, it is indirectly proportional to amounts of L and f_s.

The following equation is valid between the voltage and current of a capacitor:

$$i_C = C\frac{dv_C}{dt} = C\frac{|V_{C,PP}|}{\Delta t} \tag{14}$$

where $V_{C,PP}$ is the voltage ripple across capacitor.

Considering the values of i_C from (1) and I_L from (7), the voltage ripple across capacitor is calculated as follows:

$$V_{C,PP} = \frac{D_{OC}(1-D_{OC})I_i}{Cf_s(1-2D_{OC})} \tag{15}$$

According to above equation, it is clear that the ripple of capacitor voltage is directly proportional to I_i and indirectly proportional to amounts of C and f_s.

5. Comparison between ECSZSIs and CZSI

In this section, the comparison results between the ECSZSIs and CZSI are given in different aspects. Fig. 6 shows the power circuit of CZSI.

According to Figs. 1 and 6 it can be seen that the Z-source network of CZSI have two inductors, two capacitors and one diode but the Z-source network of ECSZSIs contains from one inductor, one capacitor, two diodes and one power switch. The less passive elements in the proposed inverters are caused to decrease in power losses, weight and volume in comparison with CZSI; whereas, the value of B_I in ECSZSIs and CZSI is equal in the same value of duty cycle. The value of voltage across input source in the proposed inverters is continuous but this value in the CZSI is discontinuous. In type I of ECSZSI, the current source has common ground with inverter stage but CZSI is not like this. The proposed inverters and CZSI have good immunity against EMI and they do not have any problem when the legs of inverter are open-circuit. Comparison results between ECSZSIs and CZSI are summarized in Table 2.

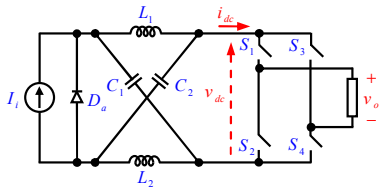

Fig. 6. Power circuit of CZSI

Table 2. Comparison of the Proposed Inverters and CZSI

		Proposed structures		CZSI
		Type I	Type II	
Number of elements	L	1	1	2
	C	1	1	2
	D	2	2	1
	S	1	1	0
B_I		$\frac{1}{1-2D_{OC}}$	$\frac{1}{1-2D_{OC}}$	$\frac{1}{1-2D_{OC}}$
Voltage across input source		Continuous	Continuous	Discontinuous
Common ground		Available	Unavailable	Unavailable

6. Simulation results

In this section, the simulation results using PSCAD/EMTDC software are shown to confirm the accuracy of presented theoretical analyses and equations. Table 3 shows the values of used parameters for simulation. The simulation results are given for type I of ECSZSI. It is noticeable that according to the analyses, the waveforms of voltages and currents in two types of the proposed inverters are same.

According to given values in Table 3 and obtained equations for current ripple of inductor and voltage ripple of capacitor, the values of inductor and capacitor can be designed. The current ripple of inductor is considered less than 5% of its average value ($I_{L,PP} \le 0.05\, I_L$). Also, the voltage ripple of capacitor is considered less than 1% of its average value ($V_{C,PP} < 0.01 V_C$). Considering these conditions and (13) and (15), the values of L and C are calculated as $L = 10\,mH$ and $C = 330\,\mu F$, respectively.

Table 3. Used Parameters in Simulation

Parameter	I_i	f_s	D_{OC}	R	$x_L\%$	$x_C\%$
Value	$3\,A$	$10kHz$	0.3	$10\,\Omega$	5%	1%

Figs. 7 to 9 show the simulation results for the proposed inverters. Fig. 7(a) shows the signals' gates of switches according to the proposed PWM method. When the value of G_S is equal to zero, the proposed inverter is in OC mode and when its value is equal to 1 the proposed inverter is in nOC mode. Fig. 7(b) shows the currents of switch S and diodes D_a and D_b. According to Fig. 7(b), it is realized that in OC mode the diodes are turned on and the switch is turned off, therefore the current of switch S is equal to zero. In nOC mode, the diodes are off; so, their currents are equal to zero.

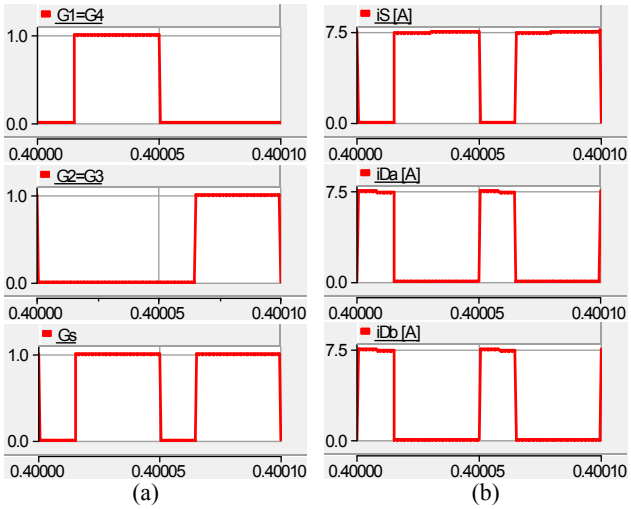

Fig. 7. (a) Signals' Gates; (b) Currents of switch S and diodes D_a and D_b

Fig. 8(a) shows the voltage and current of inductor. According to (7) and Table 3, the value of I_L is 7.5A and the obtained value from Fig. 8(a) is close to 7.5A. The value of $I_{L,PP}$ from (13) is equal to 0.197A and its value from Fig. 8(a) is close to 0.2A. Also in OC mode and according to Fig. 8(a), the value of v_L is approximately -132V that has small difference with calculated value from (2). The value of voltage across the inductor in nOC mode is obtained from difference between v_{dc} and V_C. The value of v_L in nOC mode from (2) is equal to 56.25V that Fig. 8(a) confirms it. Fig. 8(b) shows the voltage and current of capacitor. According to (11) and Table 3, the average voltage across capacitor is equal to 131.25V which is close to 132V obtained from Fig. 8(b). The voltage ripple of capacitor from (15) is 0.477V and from Fig. 8(b) is approximately 0.48V. According to Fig. 8(b), the current of capacitor in OC mode is equal to sum of I_i and I_L that the correctness of (1) is confirmed. By considering Fig. 8(b), the value of i_C in nOC is obtained from difference of I_i and I_L that the correctness of (1) is confirmed. The current of diodes

D_a and D_b in OC mode and the current of switch S in nOC mode are equal to the current of inductor L that Figs. 7(b) and 8(a) confirm them.

The voltages and currents of dc-link and output voltage and current are shown in Figs. 9(a) and 9(b), respectively. In OC mode, the dc-link current and output current are equal to zero but in nOC mode the current of them are equal to the current of inductor. The value of dc-link voltage according to (6) is equal to the value of V_C that its value from Fig. 9(a) is equal to 132V. In nOC mode, the value of output voltage from (10) is equal to 75V and according to Fig. 9(b) the similar value is obtained by simulation results. In nOC mode, the value of dc-link voltage is equal to the value of output voltage and Figs. 9(a) and 9(b) are reconfirmed it. In general, there are good agreement between the simulation and theoretical results.

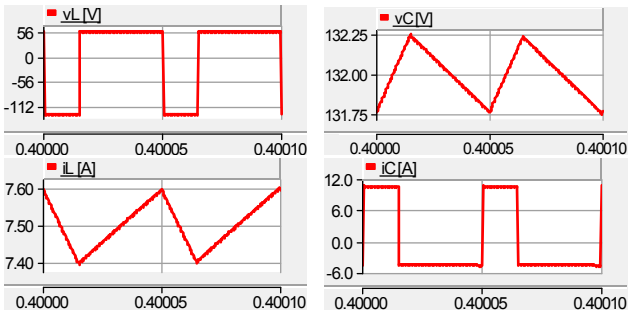

(a) (b)

Fig. 8. (a) Voltage and current waveforms of the inductor; (b) Voltage and current waveforms of the capacitor

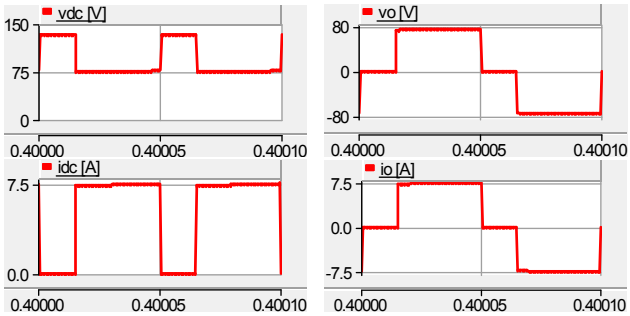

(a) (b)

Fig. 9. (a) Waveforms of dc-link voltage and current; (b) Waveforms of output voltage and current

7. Conclusion

In this paper, two new structures for current-fed Z-source inverters were proposed. Despite of the Z-source inverters with voltage source, the proposed inverters can increase the level of current with open-circuit of legs. The proposed inverters have two operating modes named OC and nOC. The complete analyses of the proposed inverters were presented in two operating modes and the voltage and current equations of all elements were calculated. The appropriate PWM method for proposed inverters was proposed and the current ripple of inductor and voltage ripple of capacitor were calculated. The current ripple of inductor has relation with the amount of load but the voltage ripple of capacitor does not have relation with the value of load. The numbers of passive elements in proposed inverters are less than CZSI but the value of current boost factor is equal in ECSZSIs and CZSI. In addition, the input voltage in the proposed inverters is continuous. The simulation results using PSCAD/EMTDC software were presented to confirm the correct operation of the proposed topologies and accuracy of the presented theories.

References

[1] F. Z. Peng, "Z-source inverter," *IEEE Trans. Ind. Appl.*, vol. 39, no. 2, pp. 504-510, Mar./Apr. 2003.

[2] E. Babaei, E. Shokati Asl, M. Hasan Babayi, and S.Laali, "Developed embedded switched-Z-source inverter," *IET Power Electron.*, vol. 9, no. 9, pp. 1828–1841, Jul. 2016.

[3] J. Anderson and F. Peng, "Four quasi-Z-source inverters," in *Proc. PESC*, 2008, Rhodes, Greece, pp. 2743-2749.

[4] E. Babaei, E. Shokati Asl, and M. Hasan Babayi, "Steady-state and small-signal analysis of high voltage gain half-bridge switched-boost inverter," *IEEE Trans. Ind. Electron.,* vol. 63, no. 6, pp. 3546-3553, June 2016.

[5] F.Z. Peng, M. Shen, and Z. Qian, "Maximum boost control of the Z-source inverter," *IEEE Trans. Power Electron.*, vol. 20, no. 4, pp. 833-838, July 2005.

[6] Y. Liu, B. Ge, and H.A. Rub, "Theoretical and experimental evaluation of four space vector modulations applied to quasi Z-source inverters," *IET Power Electron.*, vol. 6, no. 7, pp. 1257-1269, Mar. 2013.

[7] M. Hasan Babayi Nozadian, E. Babaei, S.H. Hosseini, and E. Shokati Asl, "Steady state analysis and design considerations of high voltage gain switched Z-source inverter with continuous input current," *IEEE Trans. Ind. Electron.,* vol. 64, no. 7, pp. 5342-5350, July 2017.

[8] Y. Huang, M. Shen, F.Z. Peng, and J. Wang, "Z-source inverter for residential photovoltaic systems," *IEEE Trans. Power Electron*., vol. 21, no. 6, pp. 1776–1782, Nov. 2006.

[9] J. Khajesalehi, K. Sheshyekani, M. Hamzeh, and E. Afjei, "High-performance hybrid photovoltaic –battery system based on quasi-Z-source inverter: application in microgrids," *IET Power Electron.*, vol. 9, no. 10, pp. 895-902, May 2015.

[10] E. Babaei and E. Shokati Asl, "A new topology for Z-source half-bridge inverter with low voltage stress on capacitors," *Electric Power Systems Research*, vol. 140, no. 10, pp. 724-734, Nov. 2016.

[11] P.C. Loh, D.M. Vilathgamuwa, C.J. Gajanayake, L.T. Wong, and C.P. Ang, "Z-source current-type inverters: digital modulation and logic implementation," *IEEE Trans. Power Electron.*, vol. 22, no. 1, pp. 169-177, Jan. 2007.

[12] P.C. Loh, C.J. Gajanayake, D.M. Vilathgamuwa, and F. Blaabjerg, "Evaluation of resonant damping techniques for Z-source current-type inverter," *IEEE Trans. on Power Electron.*, vol. 23, no. 4, pp. 2035-2043, July 2008.